

## CIRCUMSTELLAR GRAINS AND THE INTRINSIC POLARIZATION OF STARLIGHT

W. J. FORREST

Department of Physics, University of California, San Diego

F. C. GILLET

Kitt Peak National Observatory

AND

W. A. STEIN

Department of Physics, University of California, San Diego; and School of Physics and Astronomy,  
 University of Minnesota

Received 1974 May 23; revised 1974 August 8

### ABSTRACT

Twenty-five long-period variable stars exhibiting intrinsic variable polarization have been monitored over the range 3.5–11  $\mu$  for several cycles. No conclusive evidence for gross changes in amount of circumstellar grains has been found. Thus circumstellar infrared emission is attributed to the total abundance of grains surrounding the star, which does not change by a large amount with time, while intrinsic polarization is attributed to more localized scattering and absorption effects. Spectrophotometry with  $\Delta\lambda/\lambda \approx 0.015$  over the 8–14  $\mu$  wavelength range of several stars with different chemical compositions indicates excess emission characteristic of 3 types of grains: (1) "blackbody" grains, (2) silicate grains, and (3) silicon carbide grains.

*Subject headings:* circumstellar shells — infrared — long-period variables — polarization

### I. INTRODUCTION

Several studies have been made of the characteristics of intrinsic polarization of light from cool stars (Dombrowskii 1970; Serkowski 1971; Shawl 1972). In an attempt to obtain further information on the origin of this polarization, Dyck *et al.* (1971) demonstrated a correlation between the observed average degree of polarization and the amount of infrared emission in excess of that due to the stellar continuum. Since the excess radiation at infrared wavelengths from cool stars has been interpreted in terms of thermal reradiation by circumstellar grains (Woolf and Ney 1969), it is likely that the intrinsic polarization of light from cool stars can be explained in terms of scattering and absorption of starlight by these grains.

The motivation for the present study lies in the characteristic of the observed intrinsic polarization of many stars to vary with time. Detailed characteristics of individual stars will be discussed in § III. Since a correlation between intrinsic polarization and excess infrared radiation has been demonstrated, a program to investigate the possibility that the excess infrared radiation might also vary with time was initiated. Multiband infrared photometry of variable stars that exhibit intrinsic polarization and excess radiation from circumstellar grains has been carried out from late 1970 to early 1974. This report summarizes the results of this observing program. In addition to the search for variability, a number of spectra of the excess radiation from circumstellar grains have been obtained at different phases for a few stars and of several other stars with widely different chemical compositions. These spectra are discussed in terms of the characteristics of the grains.

### II. THE OBSERVING PROGRAM

Table 1 summarizes the stars observed in this study. In addition to the star name, the spectral type, variability class, and period are summarized from Kukarkin *et al.* (1969). The day of zero phase [ $D_0(0)$ ] is shown in column (7) as determined from the AAVSO visual light curves supplied by Mayall (1973). The phase of observation for the light curves is determined independently for each cycle from the visual light curves supplied by the AAVSO. For each cycle  $N$ , a zeroth day  $D_0(N)$  and a period  $P(N)$  is determined. Then the phase corresponding to day  $D$  is given by

$$\phi(N) = \frac{D - D_0(N)}{P(N)}. \quad (1)$$

Typically, the periods varied less than 10 percent from the average period  $P$  given in table 1, so an approximate expression for the adopted phases is

$$\phi(N) \sim \frac{D - D_0(0)}{P} - N. \quad (2)$$

The convention used for denoting different cycles in all the light curves will be

|             |    |    |    |    |    |   |   |   |   |   |
|-------------|----|----|----|----|----|---|---|---|---|---|
| N.....      | -5 | -4 | -3 | -2 | -1 | 0 | 1 | 2 | 3 | 4 |
| Symbol..... | ★  | ◇  | □  | ▲  | ●  | × | ○ | △ | □ | ◇ |

and time increases with increasing cycle number. The actual day of any particular observation at a given phase can be retrieved approximately by using eq. (2) and the  $D_0(0)$  in table 1. In column (8) the range of visual magnitude is summarized, and the range of 3.5- $\mu$  magnitude observed is shown in column (9).

TABLE 1  
STARS INCLUDED IN THE OBSERVING PROGRAM

| Name (1) | HD (2) | IRC (3) | Spectrum (4)   | Variability (5) | Period (days) (6) | $D_0(0)$ (JD 2,440,000+) (7) | Visual Magnitude (8) | $[3.5 \mu]^*$ (9) | $[4.9 \mu] - [3.5 \mu]^*$ (10) | $[8.4 \mu] - [3.5 \mu]^*$ (11) | $[11 \mu] - [3.5 \mu]^*$ (12) | $[11 \mu] - [8.4 \mu]^*$ (13) |
|----------|--------|---------|----------------|-----------------|-------------------|------------------------------|----------------------|-------------------|--------------------------------|--------------------------------|-------------------------------|-------------------------------|
| o Cet    | 14386  | 00030   | M5e-M9e        | M               | 331.7             | 820                          | 3.7-9.2              | -3.48, -2.83      | -0.30 ± 0.05                   | -0.90 ± 0.06                   | -1.68 ± 0.08                  | -0.76 ± 0.06                  |
| Z Eri    | 17491  | -10040  | M4 III         | SRb             | 80 (746)          | ...                          | 6.4-7.8              | +0.10, +0.26      | +0.17 ± 0.07                   | -0.28 ± 0.10                   | -1.04 ± 0.11                  | -0.76 ± 0.10                  |
| W Per    | 237008 | +60097  | M5             | SRb             | 469               | ...                          | 8.7-11.8             | -1.57, -1.30      | -0.15 ± 0.05                   | -1.00 ± 0.10                   | -2.58 ± 0.10                  | -1.56 ± 0.10                  |
| R Lep    | 31996  | -10080  | C7e            | M               | 432.5 (40 yr)     | 800                          | 6.8-9.6              | -1.23, -0.68      | -0.30 ± 0.10                   | -1.20 ± 0.10                   | -1.90 ± 0.10                  | -0.66 ± 0.05                  |
| Y Tau    | 38307  | +20121  | C7e            | SRa             | 240.9 (1750)      | ...                          | 6.8-9.2              | -0.40, -0.15      | -0.04 ± 0.04                   | -0.76 ± 0.06                   | -1.46 ± 0.10                  | -0.67 ± 0.07                  |
| U Ori    | 39816  | +20127  | M6e-M8e        | M               | 372.5             | 782                          | 6.3-12.0             | -1.70, -1.00      | -0.35 ± 0.05                   | -0.90 ± 0.10                   | -1.70 ± 0.15                  | -0.78 ± 0.10                  |
| TV Gem   | 42475  | +20134  | M1 Iab         | SRc             | 182               | ...                          | 6.6-8.0              | +0.50, +0.66      | -0.10 ± 0.08                   | -0.92 ± 0.08                   | -1.90 ± 0.09                  | -0.97 ± 0.04                  |
| UU Aur   | 46687  | +40158  | C5             | SRb             | 235 (3500)        | ...                          | 5.1-6.8              | -1.28, -1.08      | +0.08 ± 0.04                   | -0.53 ± 0.04                   | -0.94 ± 0.06                  | -0.42 ± 0.04                  |
| R Gem    | 53791  | +20171  | S3, 9e-S6, 9e  | M               | 369.6             | 728                          | 7.1-13.5             | +1.12, +2.04      | -0.24 ± 0.05                   | -0.88 ± 0.05                   | -1.22 ± 0.18                  | -0.30 ± 0.20                  |
| R Cnc    | 69243  | +10185  | M6e-M8e        | M               | 361.7             | 595                          | 6.8-11.2             | -1.35, -0.90      | -0.40 ± 0.08                   | -0.82 ± 0.10                   | -1.30 ± 0.10                  | -0.48 ± 0.08                  |
| R LMi    | 84346  | +30215  | M7e-M8e        | M               | 372.3             | 610                          | 7.1-12.6             | -1.35, -0.80      | -0.40 ± 0.08                   | -0.92 ± 0.06                   | -1.70 ± 0.10                  | -0.72 ± 0.05                  |
| R Leo    | 84748  | +10215  | M6.5e-M9e      | M               | 312.6             | 740                          | 5.8-10.0             | -3.23, -2.68      | -0.30 ± 0.07                   | -0.75 ± 0.10                   | -1.48 ± 0.10                  | -0.72 ± 0.05                  |
| V Hya    | 115898 | -20218  | C6e            | SRa             | 529 (18 yr)       | ...                          | 6.0-12.5             | -1.90, -1.50      | -0.52 ± 0.05                   | -1.75 ± 0.08                   | -2.30 ± 0.05                  | -0.55 ± 0.06                  |
| V CVn    | 117287 | +50276  | M4e-M6e        | SRa             | 191.9             | ...                          | 6.8-8.8              | +0.66, +0.80      | -0.27 ± 0.07                   | -1.16 ± 0.10                   | -2.22 ± 0.08                  | -1.07 ± 0.09                  |
| R Hya    | 141826 | -20254  | M6e-M8e(S)     | M               | 388.0             | 875                          | 4.5-9.5              | -3.04, -2.68      | -0.05 ± 0.05                   | -0.55 ± 0.07                   | -1.15 ± 0.10                  | -0.60 ± 0.10                  |
| S CrB    | 136753 | +30272  | M6e-M8e        | M               | 360.4             | 640                          | 7.3-12.9             | -0.75, -0.37      | -0.35 ± 0.10                   | -1.20 ± 0.15                   | -2.20 ± 0.20                  | -0.92 ± 0.10                  |
| R CrB    | 141527 | ...     | cFpep          | R CrB           | ...               | ...                          | 5.8-14.8             | +1.27, +2.95      | -1.05 ± 0.25                   | -2.32 ± 0.48                   | -2.64 ± 0.60                  | -0.30 ± 0.10                  |
| X Her    | 144205 | +40273  | C6,2e          | M               | 357.8             | 930                          | 7.5-11.0             | +0.40, +1.28      | -0.65 ± 0.10                   | -1.25 ± 0.15                   | -1.94 ± 0.15                  | -0.65 ± 0.06                  |
| U Her    | 148206 | +20298  | M6.5e-M8e      | SRb             | 95.0 (746)        | ...                          | 6.3-7.4              | -1.71, -1.63      | -0.04 ± 0.07                   | -0.55 ± 0.05                   | -1.36 ± 0.05                  | -0.80 ± 0.06                  |
| T Dra    | ...    | +60255  | C8e            | M               | 405.4             | 920                          | 7.5-12.5             | -1.24, -0.65      | -0.40 ± 0.05                   | -0.90 ± 0.10                   | -1.75 ± 0.06                  | -0.82 ± 0.08                  |
| x Cyg    | 187796 | +30395  | S7, Ie-S10, 1e | M               | 421.7             | 995                          | 9.6-12.3             | -0.30, +0.64      | -0.83 ± 0.08                   | -1.86 ± 0.14                   | -2.42 ± 0.16                  | -0.60 ± 0.05                  |
| RW Cyg   | ...    | +40424  | M3Ia           | M               | 406.8             | 890                          | 5.2-13.4             | -3.20, -2.42      | -0.12 ± 0.10                   | -0.70 ± 0.15                   | -1.40 ± 0.20                  | -0.70 ± 0.06                  |
| V Cyg    | ...    | +50338  | C7,4e          | SRc             | 586               | ...                          | 7.7-9.4              | -0.04, +0.10      | 0.0 ± 0.04                     | -0.92 ± 0.06                   | -2.63 ± 0.08                  | -1.71 ± 0.09                  |
| R Cas    | 244490 | +50484  | M6e-M8e        | M               | 421.3             | 650                          | 9.1-12.8             | -1.65, -0.83      | -0.83 ± 0.08                   | -1.80 ± 0.15                   | -2.41 ± 0.15                  | -0.60 ± 0.06                  |
|          |        |         |                |                 | 431.0             | 610                          | 7.0-12.6             | -2.84, -2.06      | -0.38 ± 0.08                   | -1.10 ± 0.10                   | -2.04 ± 0.10                  | -0.92 ± 0.06                  |

\* Quoted values represent those results actually observed. None of the stars were observed through all phases of variability.

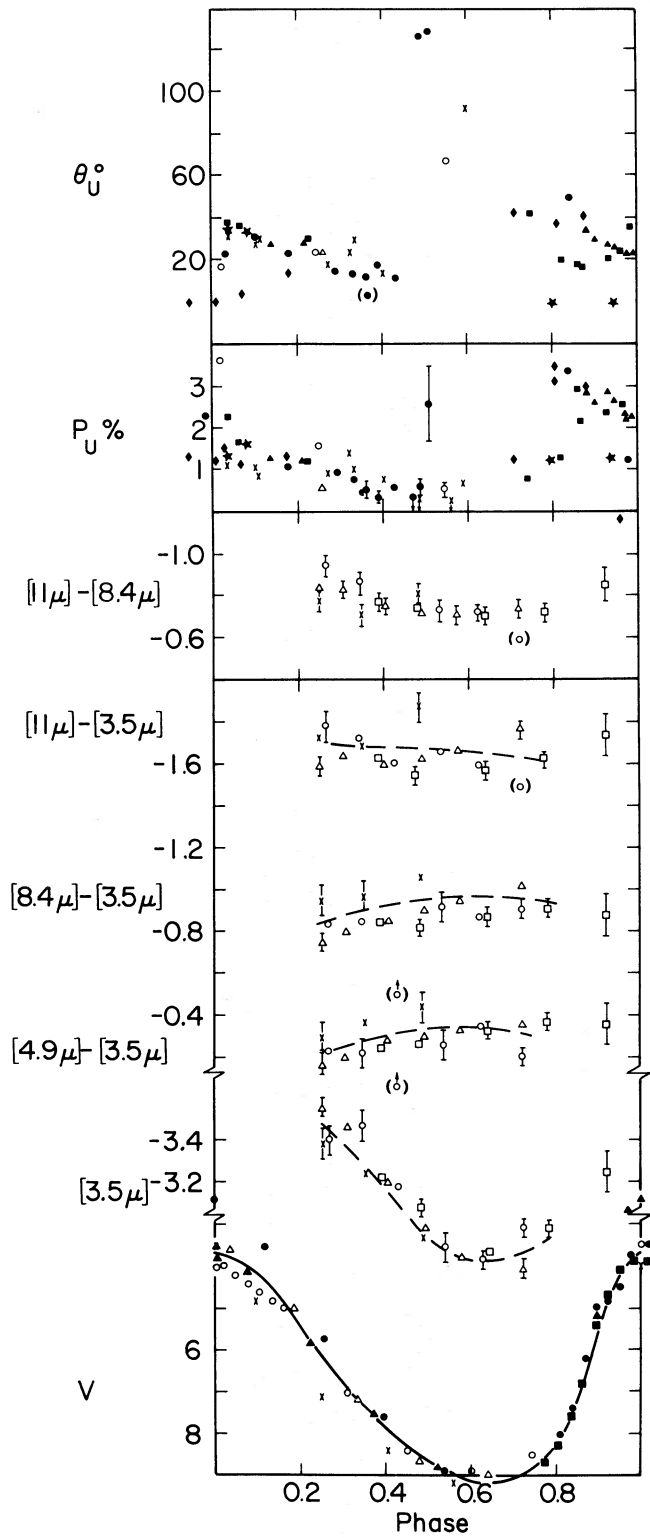


FIG. 1.—Polarization and photometric data on  $\circ$  Cet

The infrared colors determined during the period of observation and limits to observed change of color are shown in columns (10)–(13). In the case of the Mira variables and R CrB the  $\pm$  numbers refer to the authors' estimates of actual variability from the mean light curves while for the semiregular variables they represent upper limits to the possible variation.

The observations consisted primarily of two types: (1) Broad-band photometry as a function of time at effective wavelengths of 3.5, 4.9, 8.4, and 11  $\mu$ —the photometric system used by Gillett, Merrill, and Stein (1971). (2) Narrow-band spectrophotometry with resolution  $\Delta\lambda/\lambda \approx 0.15$  over the wavelength range 8–14  $\mu$ . This spectral region is of particular importance because the emissivity of some solid grain materials exhibits identifiable structure at these wavelengths.

### III. PHOTOMETRIC LIGHT CURVES

Only selected examples of data obtained on the stars listed in table 1 are discussed in detail here. Data on polarization of the stars are also included to the extent of the availability of this information. The results will be compared with those expected for a hypothetical variable star in § IV.

#### a) $\alpha$ Ceti (Mira)

Data on observed flux and polarization of  $\alpha$  Ceti as a function of phase is shown in figure 1. Different symbols indicate observations obtained during different cycles as described in § II. Percentage polarization and position angle at the  $U$  wavelength have been obtained from Serkowski (1966, 1971a, 1974), Shawl (1972), Zappala (1967), Kruszewski, Gehrels, and Serkowski (1968), and Dyck and Shawl (1972). Mira exhibits a remarkably sharp increase in percent polarization at phase 0.8 that appears to occur each cycle (Shawl 1971, 1972).

The "mean visual light curve" (solid line, Campbell 1955) together with current AAVSO visual estimates (Mayall 1973) are shown along with 3.5- $\mu$  magnitude and the observed colors [4.9  $\mu$ ] – [3.5  $\mu$ ], [8.4  $\mu$ ] – [3.5  $\mu$ ], [11  $\mu$ ] – [3.5  $\mu$ ], and [11  $\mu$ ] – [8.4  $\mu$ ] as obtained in this study ([ $\lambda_n$ ] designates the observed magnitude at the wavelength  $\lambda_n$ ). Typical error bars are shown on several of the points. The photometric coverage in phase of  $\alpha$  Ceti is limited somewhat by the period of time that the star was available as a nighttime object.

It is significant that while the polarization, visual light, and light at 3.5  $\mu$  change considerably with phase, the infrared colors are constant to within  $\pm 10$  percent or  $\pm 0.1$  mag. The infrared colors of  $\alpha$  Ceti before and after 0.8 phase are of particular interest because of the sharp polarization increase at that phase. Although it was not possible to obtain a large amount of coverage during this critical period, the data that were obtained indicate only a possible small continuous slow change of infrared colors through the period before and after 0.8 phase.

#### b) R Leonis

The characteristics of percentage polarization and position angle of polarization for R Leo are summarized in figure 2 from the work of Serkowski (1966, 1971b, 1974), Dyck and Shawl (1972), Kruszewski *et al.* (1968), and Dyck and Sanford (1971). One of the interesting characteristics of the polarization of this star (among others) is the rapid change in position angle of polarization ( $\theta_B = 160^\circ - 110^\circ$ ) during a period when the percentage polarization changed from  $P_B = 3.7$  percent to  $P_B = 1$  percent.

Although the visual light and 3.5- $\mu$  radiation vary by a large amount, no large changes appear to occur in the [11  $\mu$ ] – [3.5  $\mu$ ] or [11  $\mu$ ] – [8.4  $\mu$ ] colors as would be expected if the amount of dust changed by a large factor during the cycle of the star.

This is one of the few stars for which infrared and polarization data were obtained over the same cycle. It is particularly interesting to note that during the period of the rapid changes in polarization described above no significant change in infrared color was observed.

#### c) R Cassiopeiae

R Cassiopeiae is an M star for which very few polarization data appear to be available. Excellent infrared coverage has been obtained during almost the entire phase of this star, and the results are shown in figure 3. Again, in spite of large visual and 3.5- $\mu$  changes of flux with phase, the infrared colors appear to show no significant change.

#### d) R Geminorum

R Geminorum is an S star for which limited polarization data are available. The polarization data are shown in figure 4 from the measurements of Vardanian (1969), Dyck (1968), and Serkowski (1974). Of particular interest is the change of  $P_v$  from 3 percent to approximately 0 percent during a period when the position angle of polarization did not significantly change. This is in contrast to one of the stars described earlier (R Leo).

The visual and 3.5- $\mu$  radiation shows large changes during the cycle of the star. This star exhibits a possible small systematic change of the color [11  $\mu$ ] – [3.5  $\mu$ ] with phase, although other colors appear unchanged.

#### e) $\chi$ Cygni

The polarization (Shawl 1972; Serkowski 1974) and infrared data on  $\chi$  Cyg are shown in figure 5. The position angle of observed polarization has changed during one series of observations by an angle of  $80^\circ$  during a small fraction of phase of the star (Serkowski 1974). During this period the percentage polarization changed very little. Infrared data were not obtained during the above event; however, good coverage with phase was obtained during other cycles of the star. In particular, the increase in  $P_B$  by more than a factor of 2 during the zeroth cycle ( $\times$ 's, fig. 5) was not

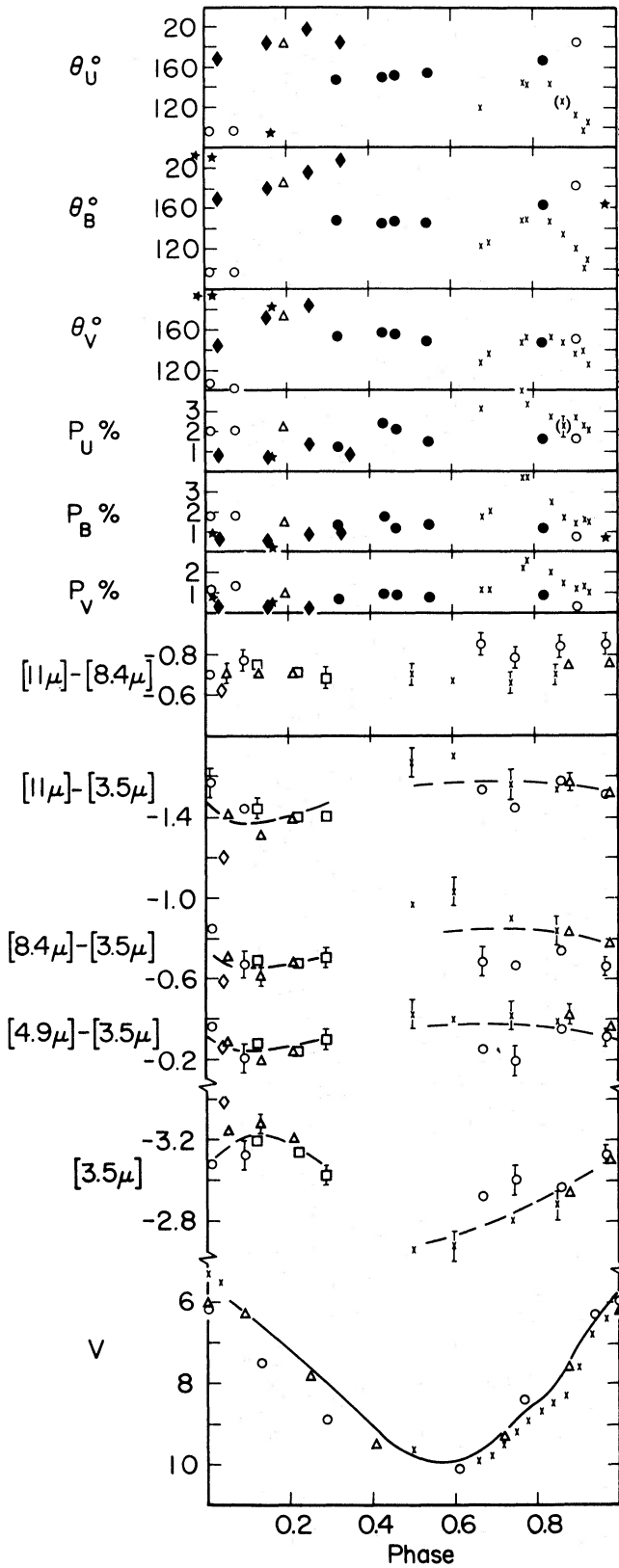


FIG. 2.—Polarization and photometric data on R Leo

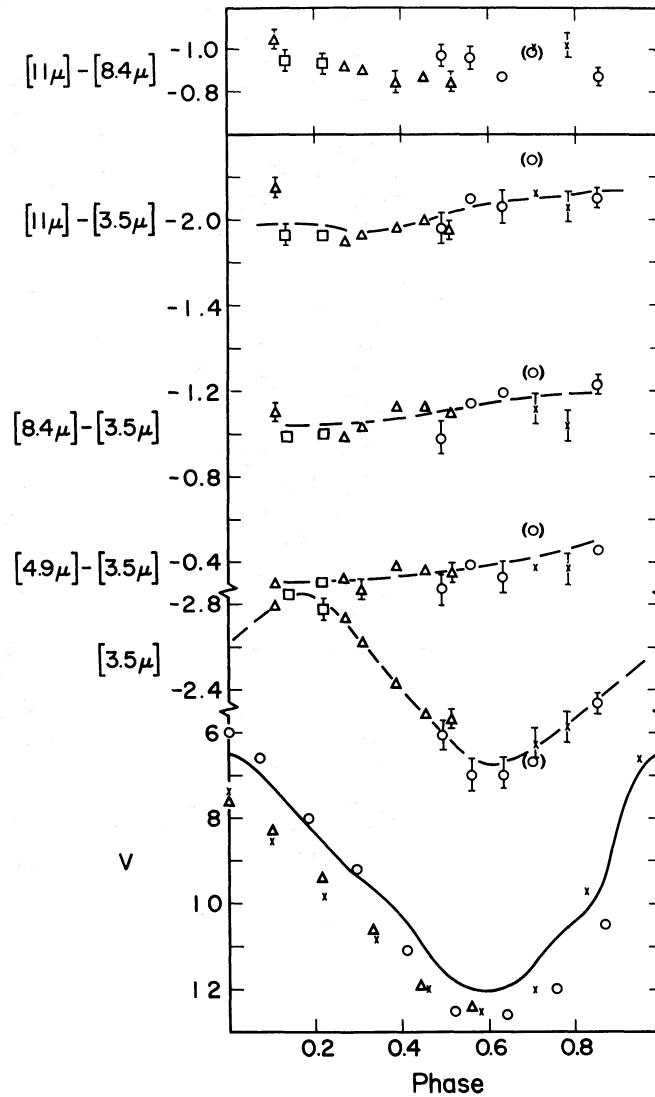


FIG. 3.—Photometric data on R Cas

accompanied by any large change in the  $[11\ \mu] - [3.5\ \mu]$  or  $[11\ \mu] - [8.4\ \mu]$  colors. A small systematic change in the  $[11\ \mu] - [3.5\ \mu]$  color appears to be evident when considering all the data. This result will be discussed further in § IV. The visual and  $3.5\text{-}\mu$  light curves of this star have been discussed in detail by Strecker (1973).

#### f) *R Leporis*

One example of the several carbon stars observed in this study (table 1) is R Lep; figure 6 summarizes these results. The polarization data are from the work of Serkowski (1966, 1971a, 1974), Kruszewski *et al.* (1968), Dyck and Sanford (1971), and Dyck and Shawl (1972). Although changes of polarization are evident during the monitoring period, no large change of any of the infrared colors was observed.

#### IV. DISCUSSION OF LIGHT CURVES

In summary: of the light curves and infrared colors obtained throughout the cycles of several variable stars, there is only one case in which the  $[11\ \mu] - [3.5\ \mu]$  color appeared to change significantly—R Gem. This change may also exist in the observed  $[11\ \mu] - [8.4\ \mu]$  color of this star, but the scatter of data points is larger. In the case of *o* Cet where a large change in polarization has been found to occur at phase 0.8, no significant change in infrared color indicative of a change of circumstellar dust abundance is evident. In other cases during which significant polarization changes have been observed (e.g., R Leo,  $\chi$  Cyg) or where significant changes in position angle of polarization have been observed (e.g., R Leo,  $\chi$  Cyg, R Lep), no large infrared color changes were seen.

In order to interpret the photometric light curves

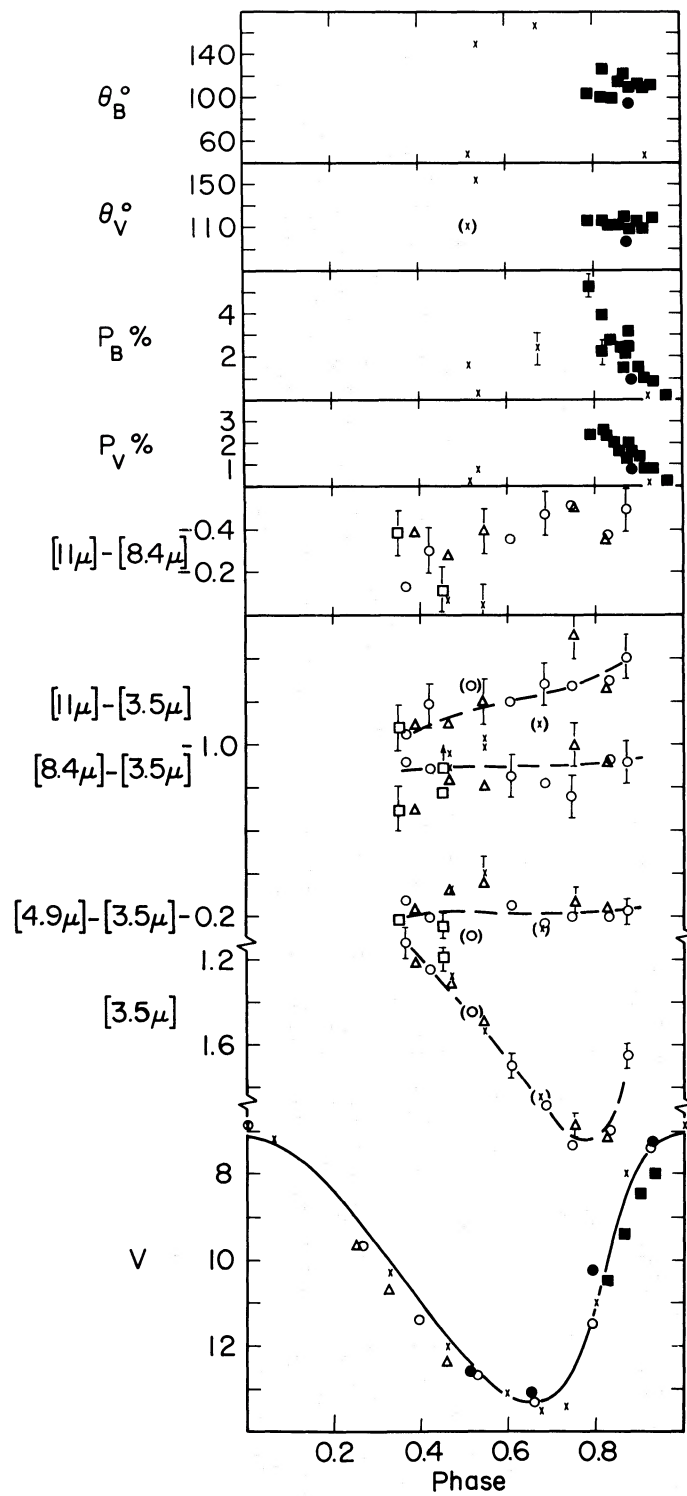


FIG. 4.—Polarization and photometric data on R Gem

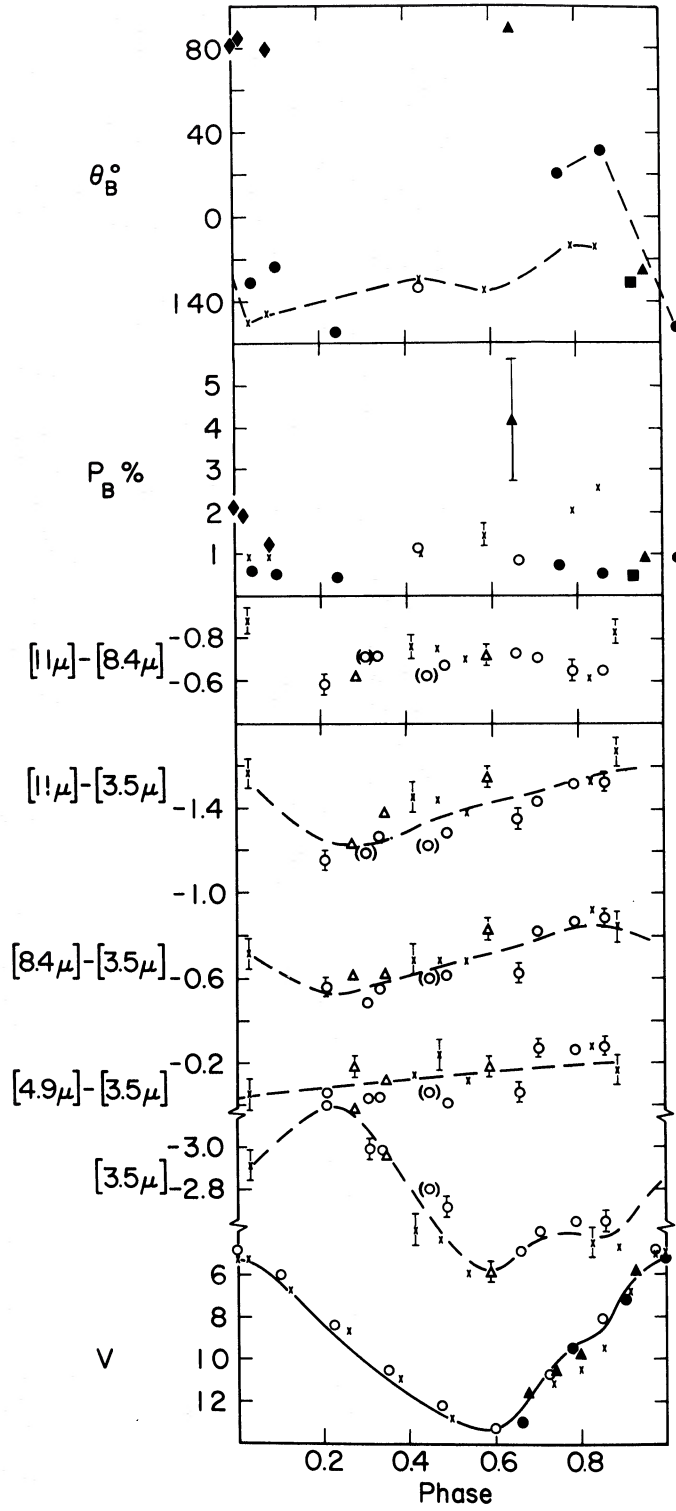


FIG. 5.—Polarization and photometric data on  $\chi$  Cyg

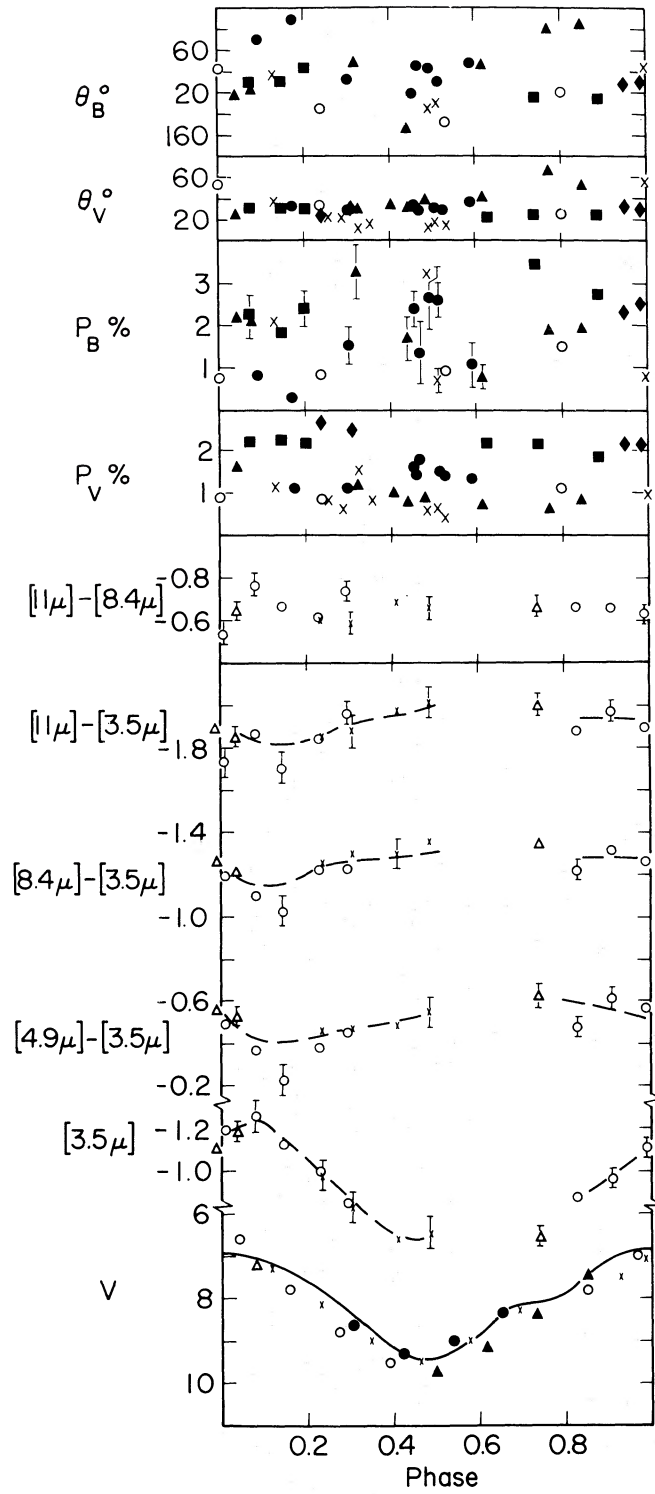


FIG. 6.—Polarization and photometric data on R Lep

obtained for the large number of stars observed, it is helpful to analyze the expected variability at infrared wavelengths of a typical hypothetical star, taking into account anticipated physical effects. Since the primary purpose of the photometric observations was to search for changes in the amount of circumstellar dust, effects that might produce a change in infrared photometric colors other than a change in amount of circumstellar dust should be taken into account.

The infrared characteristics of the hypothetical star were deduced from a model star having variability

similar to  $\chi$  Cyg. If the amount of circumstellar dust remained constant with time, it is expected that some change in the infrared colors of the star would still occur. Two effects are of primary interest:

1) The luminosity and temperature of variable stars change with time. Since more energy is available to heat circumstellar grains when the luminosity of the star is large, the flux of radiation from the grains at infrared wavelengths may be observed to change even though the amount of circumstellar dust is constant. Also, since the emission from dust occurs

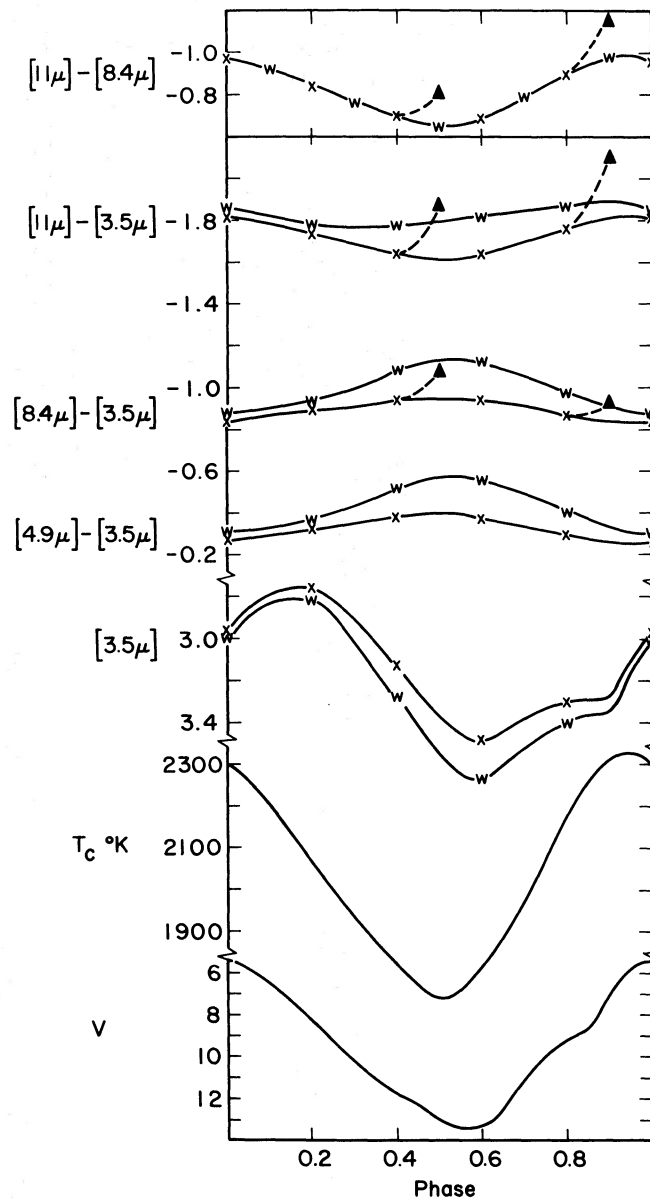


FIG. 7.—Characteristics of a hypothetical variable star surrounded by circumstellar dust. The curves are, from the bottom, the mean visual light curve for  $\chi$  Cyg (Campbell 1955), the mean  $1.04 \mu - 3.5 \mu$  color temperature,  $T_c$ , for  $\chi$  Cyg (Strecker 1973), and the infrared magnitudes and colors for the hypothetical star as described in the text versus visual phase. The curves labeled *W* include the possible effect of  $H_2O$  absorption at  $3.5 \mu$ , and the solid triangles indicate the expected change in the infrared due to a 50% increase in the amount of silicate dust.

at wavelengths longward of the peak stellar luminosity, changes in the temperature of the star may result in changes in the contrast of the grain emission relative to the stellar continuum, and this will be observed in the infrared colors. Finally, the energy distribution of the dust emission will depend on dust temperature which may vary with the stellar luminosity.

2) Molecular absorption in the stellar atmosphere will vary in strength as the abundance of the molecule changes. This molecular absorption might be periodically variable as the physical conditions in the stellar atmosphere change.

The hypothetical star has been constructed by adding grain emission having a spectral dependence as seen in the Trapezium (fig. 10 of Ney, Strecker, and Gehrz 1973) to the radiation from the star. The star is initially assumed to radiate as a blackbody with temperature given by the  $1.04\ \mu - 3.5\ \mu$  color temperature, and the grains are constrained to radiate a constant fraction equal to 0.02 of the total luminosity, typical of the M and S stars here, with the grain temperature varying as (stellar luminosity)<sup>1/4</sup>.

Figure 7 shows the visual light curve (Campbell 1955) and the  $1.04\ \mu - 3.5\ \mu$  color temperature as a function of phase (Strecker 1973) for  $\chi$  Cyg; and the  $3.5\text{-}\mu$  magnitude  $[3.5\ \mu]$  and the expected photometric colors  $[4.9\ \mu] - [3.5\ \mu]$ ,  $[8.4\ \mu] - [3.5\ \mu]$ ,  $[11\ \mu] - [3.5\ \mu]$ ,  $[11\ \mu] - [8.4\ \mu]$  of the hypothetical star assuming no change in the abundance of circumstellar dust. The photometric color changes that occur with the phase of this hypothetical star are produced entirely by the luminosity and temperature changes of the star.

The effect of molecular opacity such as that of  $\text{H}_2\text{O}$  on the stellar continuum is less certain. Spectra obtained by Woolf, Schwarzschild, and Rose (1964) of M-type Mira variable showed strong absorption bands (centered at 1.4, 1.9, and  $2.7\ \mu$ ) which were attributed to the opacity of hot water vapor. The  $3.5\text{-}\mu$  magnitude will be affected by absorption in the wings of the  $2.7\text{-}\mu$   $\text{H}_2\text{O}$  band. In addition, Frogel (1971), from spectra taken in the  $2.0\text{--}2.5\ \mu$  region, has observed changes in the  $\text{H}_2\text{O}$  absorption at  $2.1\ \mu$  in the wings of the  $1.9\text{-}\mu$   $\text{H}_2\text{O}$  band for several M-type Mira variables in common with this program. He observed that maximum  $\text{H}_2\text{O}$  absorption came at visual and temperature minimum and vice versa. An empirical approach has been adopted to estimate the possible effect of this variation on the observed  $3.5\text{-}\mu$  broad-band magnitudes. The available spectra of M-type Mira variables indicate an absorption feature for  $\lambda \lesssim 3.5\ \mu$  which has been attributed to  $\text{H}_2\text{O}$  absorption (Woolf *et al.* 1964; Gillett, Low, and Stein 1968). Comparison with the measurements of Frogel (1971) on the same stars indicates that the depression at  $2.1\ \mu$  approximately equals the depression at  $3.25\ \mu$ . This approximation is taken to be an equality, and the effect of a given  $3.25\text{-}\mu$  depression on the observed  $3.5\text{-}\mu$  magnitude ( $\lambda \approx 3.0\text{--}4.0\ \mu$ ) is determined from the observed shape of the available spectra in the  $3.0\text{--}4.0\ \mu$  region of M-type Mira variables. The  $2.1\text{-}\mu$   $\text{H}_2\text{O}$  absorption data of Frogel (1971) for all M

stars in common with this program were plotted versus phase and averaged, and the effect of this average absorption on the  $3.5\text{-}\mu$  magnitude was applied to the hypothetical star of figure 7. Other possible stellar opacity effects, such as  $\text{H}_2\text{O}$  absorption at longer wavelengths and CO absorption in the  $4.9\text{-}\mu$  band, have not been included for this star.

The observed flux and color dependence on phase should be compared with the anticipated results as calculated for the hypothetical variable star shown in figure 7. The observed infrared brightness and infrared colors of variable stars generally show less change than that of figure 7 in which the anticipated effects of changes in the luminosity and temperature of the star and water vapor absorption are included as discussed above. The expected  $[11\ \mu] - [8.4\ \mu]$  color should be quite independent of possible water-vapor absorption effects and is therefore a good indicator of excess dust emission—at least for those M stars exhibiting silicate emission or those carbon stars with silicon carbide emission. The expected  $[11\ \mu] - [8.4\ \mu]$  color decreases toward minimum light of the hypothetical variable star (fig. 7); however, the observed  $[11\ \mu] - [8.4\ \mu]$  color generally shows little change. This might be some indication that on the average there is a small increase in dust emission of M and S stars during minimum light of about a factor 1.5–1.8. This possibility should probably be investigated further. We do not, however, consider the lack of  $[11\ \mu] - [8.4\ \mu]$  color change for observed stars, in comparison with an expected small decrease in this color due to the stellar luminosity and temperature change alone, to be conclusive evidence of a change in the amount of circumstellar dust through the cycle of variable stars.

## V. SPECTRAL ENERGY DISTRIBUTIONS

During the course of this observational program the infrared spectral energy distribution between 8 and  $14\ \mu$  was obtained for a number of stars with a resolution  $\Delta\lambda/\lambda \approx 0.015$  utilizing the cooled variable-bandpass filter wheel system described by Gillett and Forrest (1973). The total flux as a function of wavelength will not be shown here for all stars observed. Of more interest is the energy distribution of the excess radiation in the  $8\text{--}14\ \mu$  range that has previously led to information about the chemical compositions of circumstellar grains. Thus most of the data to be discussed here consist of the wavelength distribution of excess radiation which has been determined by subtraction of a blackbody continuum from the total observed radiation. The procedure adopted for the M and S stars was to fit the short-wavelength broad-band measurements ( $[2.3\ \mu]$ ,  $[3.5\ \mu]$ , and  $[4.9\ \mu]$ ) by trial and error with a blackbody of temperature appropriate to the star's spectral type and consistent with the observed fluxes, taking into account possible depressions due to stellar CO and  $\text{H}_2\text{O}$  in these bands. This blackbody continuum was then assumed to represent the flux from the star in the  $\lambda \approx 8\text{--}14\ \mu$  window and subtracted to derive the excess. The

blackbody temperatures adopted are given in the figure legends.

Figure 8 shows the spectral energy distribution of excess radiation from several M-type Mira stars. The stars are:  $\circ$  Cet, R Cas, U Her, U Ori, R LMi, and R Leo. The excess radiation from all of these stars shows the silicate type distribution similar to that observed for other M stars (Gillett *et al.* 1968; Gammon, Gaustad, and Treffers 1972) and the Orion Trapezium region (Stein and Gillett 1969). Errors in

flux level associated with individual points are consistent with the degree of scatter of the data. A spectrum of RX Boo (M7e-M8e) has been obtained (not shown in this paper) which does not confirm the absorption feature at  $\lambda \sim 11.5 \mu$  referred to by Hackwell (1972). It is interesting to note that not all of these "silicate type" distributions are identical. Some appear to show a somewhat more sharply increasing distribution in the 8-9.5  $\mu$  range and a more slowly decreasing distribution at wavelengths larger

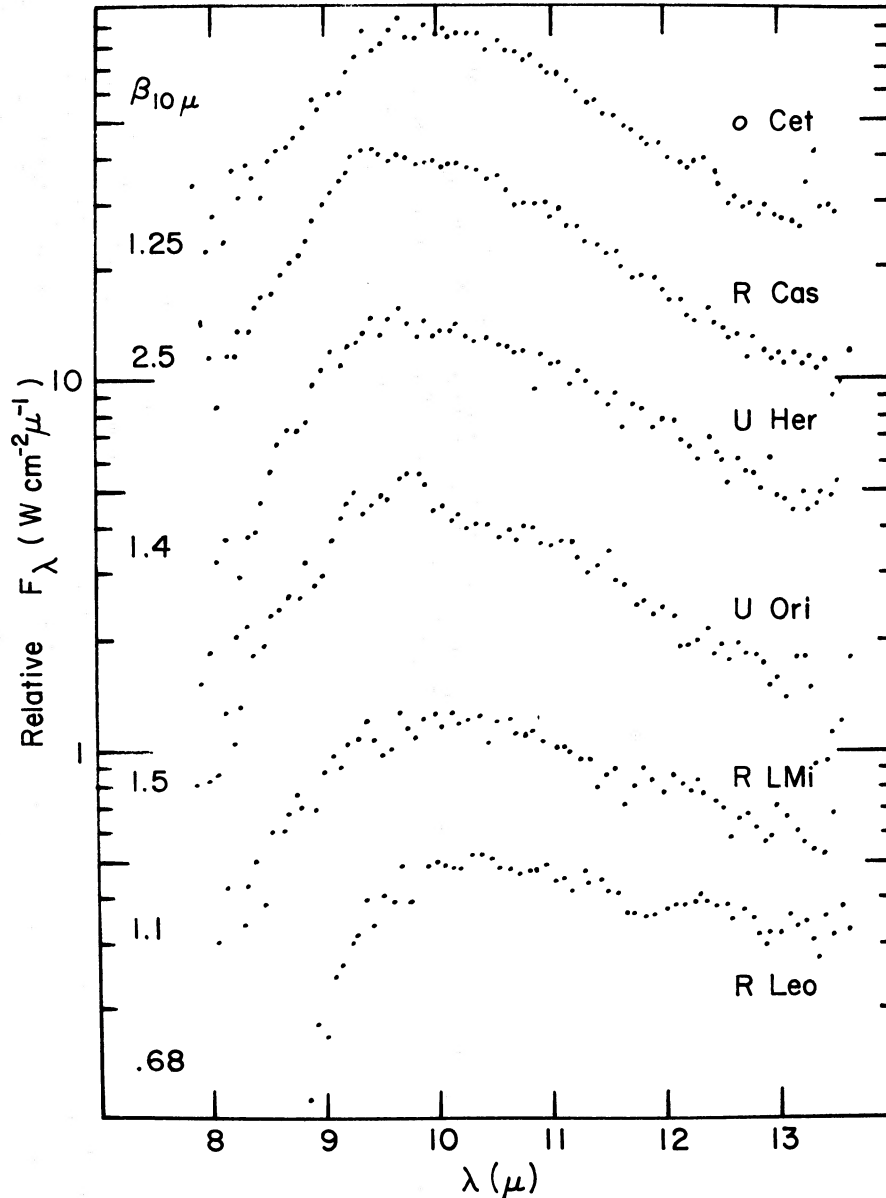


FIG. 8.—Spectral energy distribution of excess emission from several M-type Mira stars. In figs. 8-13 the "relative flux" represents the actual flux normalized by an arbitrary constant for convenient display. The fractional amount of excess relative to the continuum is given by  $\beta_{\lambda} \equiv [F_{\lambda}(\text{total}) - F_{\lambda}(\text{continuum})]F_{\lambda}^{-1}(\text{continuum})$ . The temperatures of the blackbodies which have been subtracted to derive the excess flux as described in the text are as follows:  $\circ$  Cet (2500° K), R Cas (2500° K), U Her (2400° K), U Ori (2400° K), R LMi (2000° K), R Leo (2500° K).

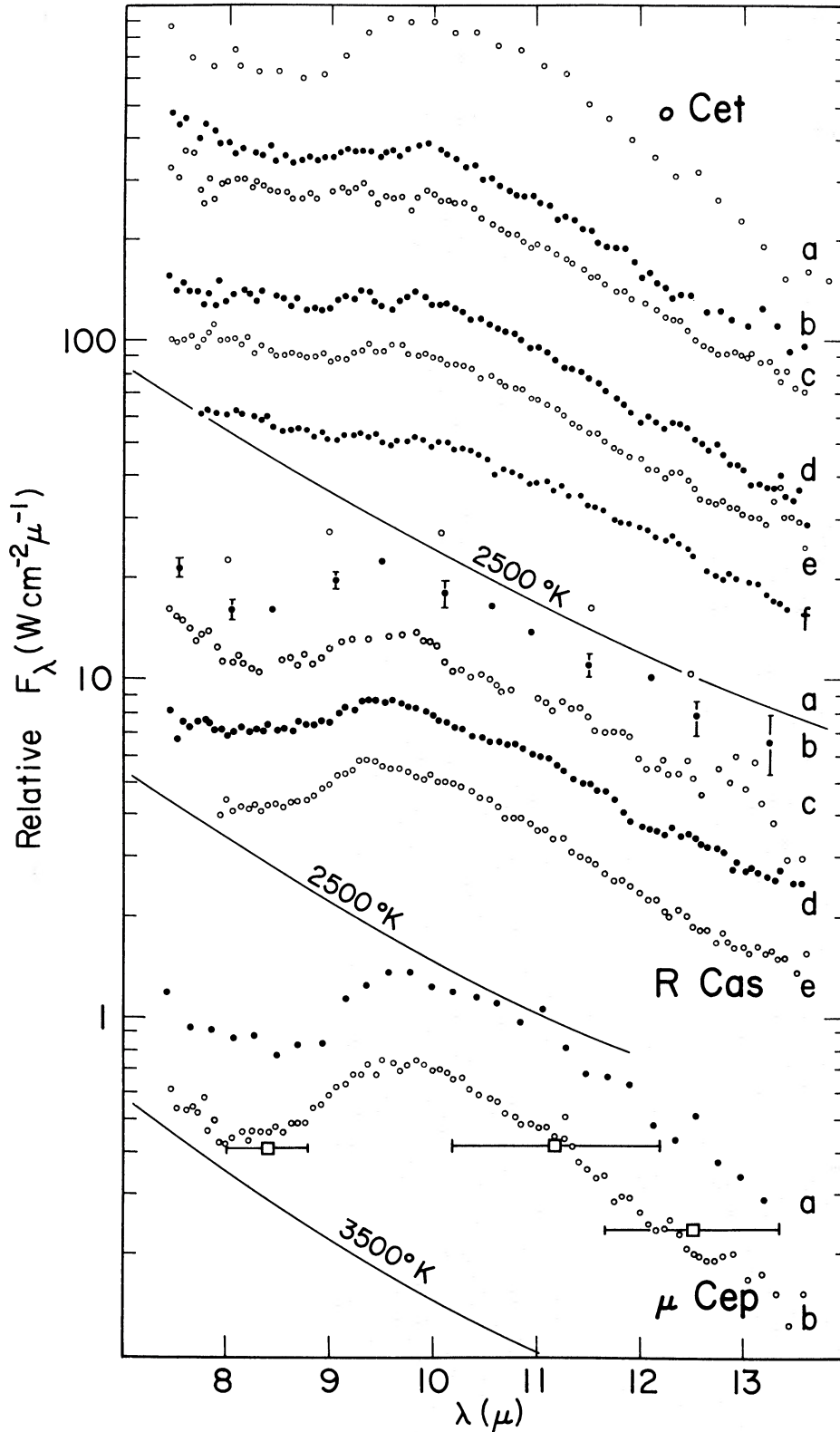


FIG. 9.—Spectral energy distribution as a function of time from  $\circ$  Ceti, R Cas, and  $\mu$  Cep. The blackbody curves are typical assumed stellar continua, referring to the spectrum just above, which would be subtracted to derive the excesses as discussed earlier. For  $\circ$  Ceti: Curve *a*, 1967 Oct. 17 (UT), phase 0.96 (−4); curve *b*, 1971 December 13, phase 0.45 (1); curve *c*, 1972 January 10, phase 0.54 (1); curve *d*, 1972 November 4, phase 0.41(2); curve *e*, 1972 December 4, phase 0.50 (2); curve *f*, 1973 December 18, phase 0.64 (3). For R Cas: Curve *a*, 1969 November 22 UT, phase 0.86 (−1); curve *b*, 1970 November 13, phase 0.71(0); curve *c*, 1971 December 17, phase 0.64(1); curve *d*, 1972 November 4, phase 0.39(2); curve *e*, 1973 September 21, phase 0.14 (3). For  $\mu$  Cep: 1967 October 17 and 1973 June 17 (UT).

than  $11 \mu$  (e.g., R Leo). This variation in detailed spectral energy distribution has also been noted by Hackwell (1971; 1972) and by Treffers and Cohen (1974).

Attempts have been made to reproduce the spectral shape of excess radiation from R Leo in terms of the spectral feature observed for material radiating in the Orion Trapezium. It has been found that effects of optical depth and/or grain temperature are not sufficient. Effects of grain size can reproduce the observed energy distribution of R Leo, but grains of a few microns in size are required. The detailed shape of the underlying stellar continuum may also be a significant effect in that it is observed that peculiar grain spectra are seen only in those stars having small excess grain radiation.

Spectra of a few stars have been obtained several times over the last few years. In figure 9 is shown the total observed flux from  $\alpha$  Cet, R Cas, and  $\mu$  Cep as a

function of wavelengths between  $8$  and  $14 \mu$  at several different times. It is clear that very little change is shown in this spectral energy distribution with time for R Cas and  $\mu$  Cep. However, it appears that there is a possibility that the strength of the silicate-type excess of  $\alpha$  Cet has been decreasing very slowly with time over the last several years, the largest change being between the early (1967) spectrum and the present series. This result is not verified by broadband photometry which is less strongly dependent on the detailed shape of the  $8$ – $14 \mu$  spectral energy distribution. It is significant that although the excess is relatively weaker at present, the spectrum of the excess derived by subtracting a blackbody continuum (fig. 8) is still similar to the flux observed from the Trapezium (fig. 10). If this change is real, it would represent a secular decrease of approximately a factor 1.5–2 in the amount of dust around  $\alpha$  Cet during the period late 1967 to late 1971.

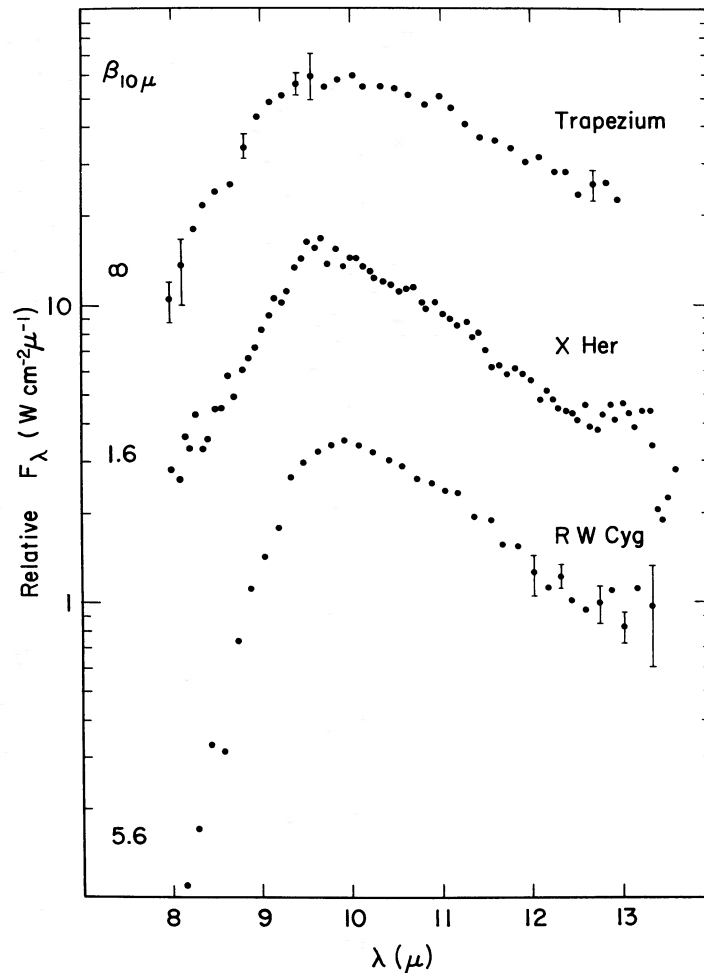


FIG. 10.—Spectral energy distribution of excess emission from M-type semiregular variable stars compared with that of the Trapezium region of the Orion Nebula. The fractional amount of excess relative to the continuum is given by  $\beta_{\lambda} \equiv [F_{\lambda}(\text{total}) - F_{\lambda}(\text{continuum})]/F_{\lambda}^{-1}(\text{continuum})$ . The temperatures of the blackbodies which have been subtracted are as follows: X Her ( $2500^{\circ}$  K), RW Cyg ( $3000^{\circ}$  K).

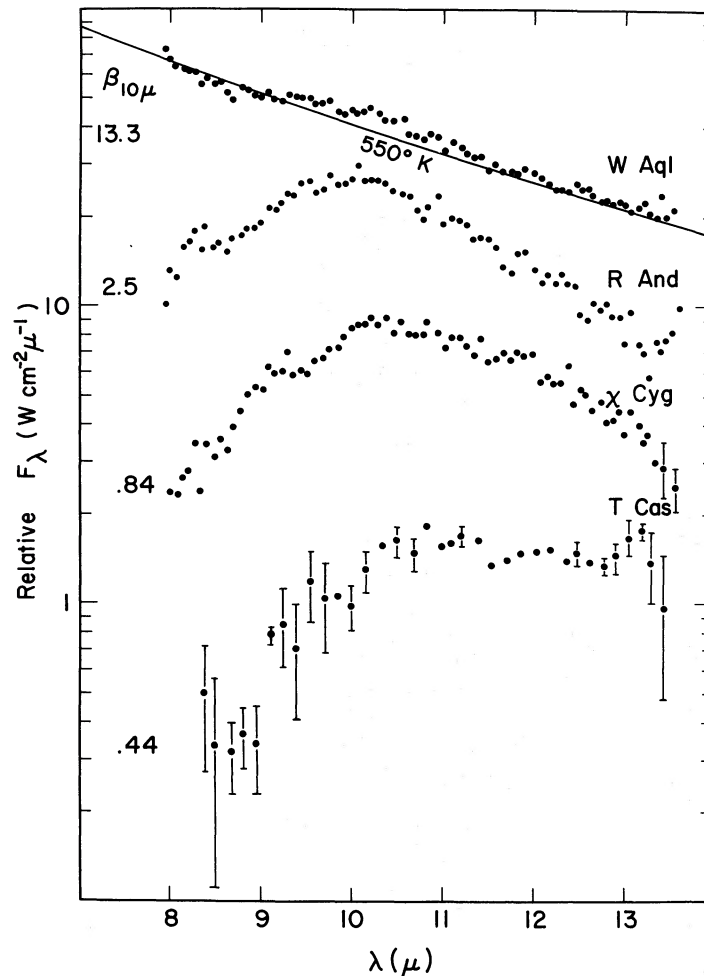


FIG. 11.—Spectral energy distribution of excess emission from S and M,S stars. The total observed flux from W Aql is plotted as discussed in the text. The spectral types of the stars, from Kukarkin *et al.* (1969), and the temperatures of the blackbodies which have been subtracted are: W Aql, S3,9e; R And, S6,6e (M73) [2000° K];  $\chi$  Cyg, S7,1e (M) [2000° K]; T Cas, M6e (S) [2500° K].

In figure 10 the spectra of the excess emission from the M-type semiregular variables X Her and RW Cyg are compared with those of the total flux from the Orion Trapezium region. The stellar excess radiation again clearly resembles that of the material radiating in Orion which has been interpreted in terms of grains of silicate material. In some cases where statistical errors are large, these errors are indicated on the data points.

The spectral energy distributions of several S and M,S stars are shown in figure 11. The energy distribution of excess radiation observed from R And,  $\chi$  Cyg, and T Cas (an Me star with S star characteristics [Spinrad and Newburn 1965]) is shown along with the total energy observed over this wavelength range from W Aql. In the case of W Aql the attempt to fit the short-wavelength energy distribution with an approximate stellar blackbody ( $T_* \sim 2000^\circ$  K) failed. Rather, the energy distribution is fitted by the sum of two blackbodies,  $T \sim 1500^\circ$  K representing the

stellar continuum, and  $T \sim 550^\circ$  K representing the excess. The ratio of excess to continuum at  $10 \mu$  is 13 on this model, so subtraction of the stellar continuum was not important. Essentially all the flux observed at these wavelengths is excess. W Aquilae is unique among the M and S stars studied here. The excess is apparently quite smooth with no large deviations from the  $\sim 550^\circ$  K blackbody which describes the energy distribution. It appears that the excess radiation from R And and  $\chi$  Cyg is typical of the silicate emissivity discussed for many other stars. The statistical errors involved in the spectrum of T Cas are larger than in many of the other stars. It is interesting to note, however, that the excess radiation from T Cas can be characterized by a relatively larger flux beyond  $12 \mu$  than many of the other typical stars exhibiting silicate-type excess radiation.

In contrast to many of the other spectra described, the energy distribution of radiation from carbon stars has quite a different character. The  $7.5\text{--}13.5 \mu$  spectra

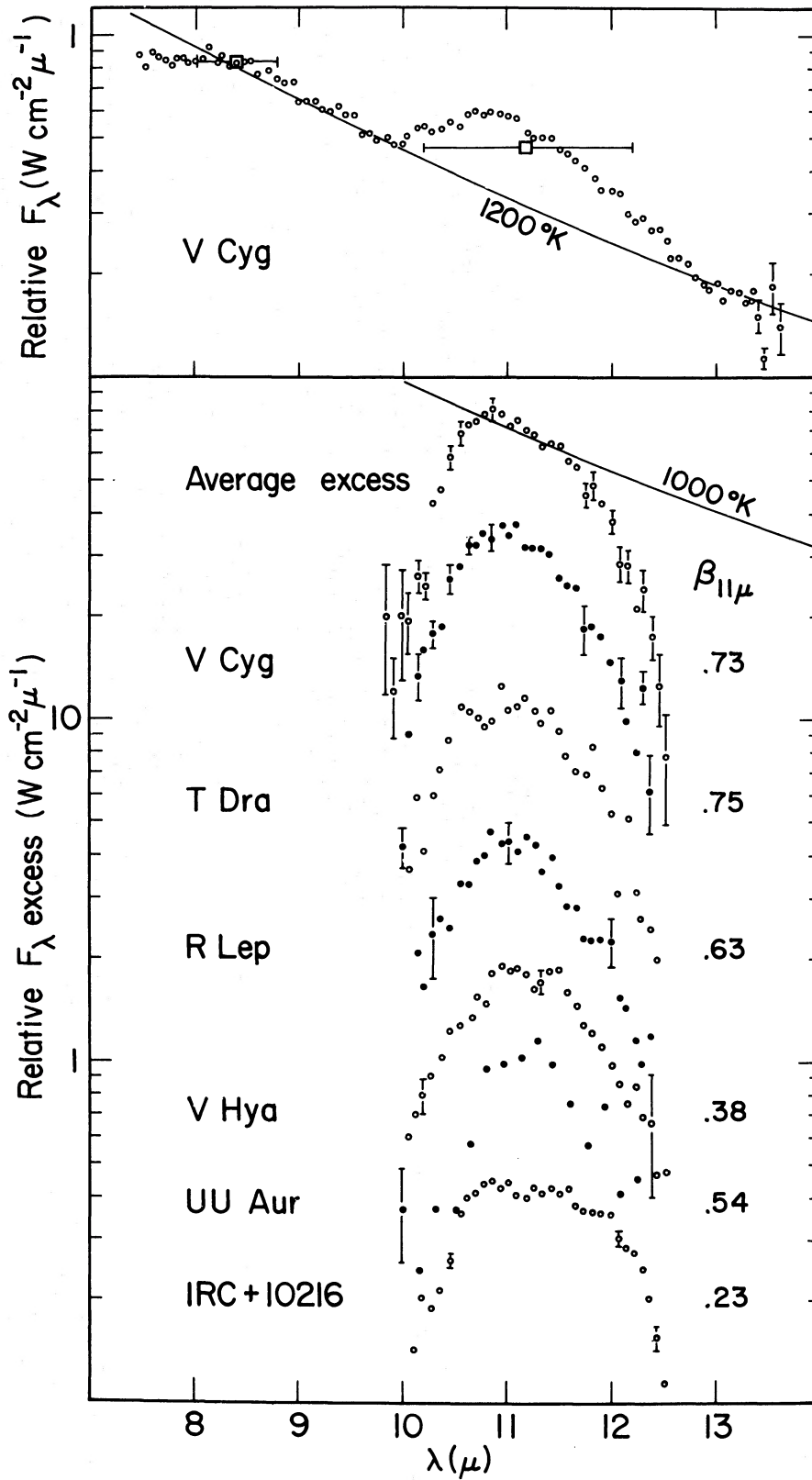


FIG. 12.—Spectral energy distribution of emission feature of carbon stars and the total flux from V Cyg. The average of the normalized excesses of V Cyg, T Dra, R Lep, and V Hya is plotted with error bars if  $\sigma/S \geq \pm 6\%$ .

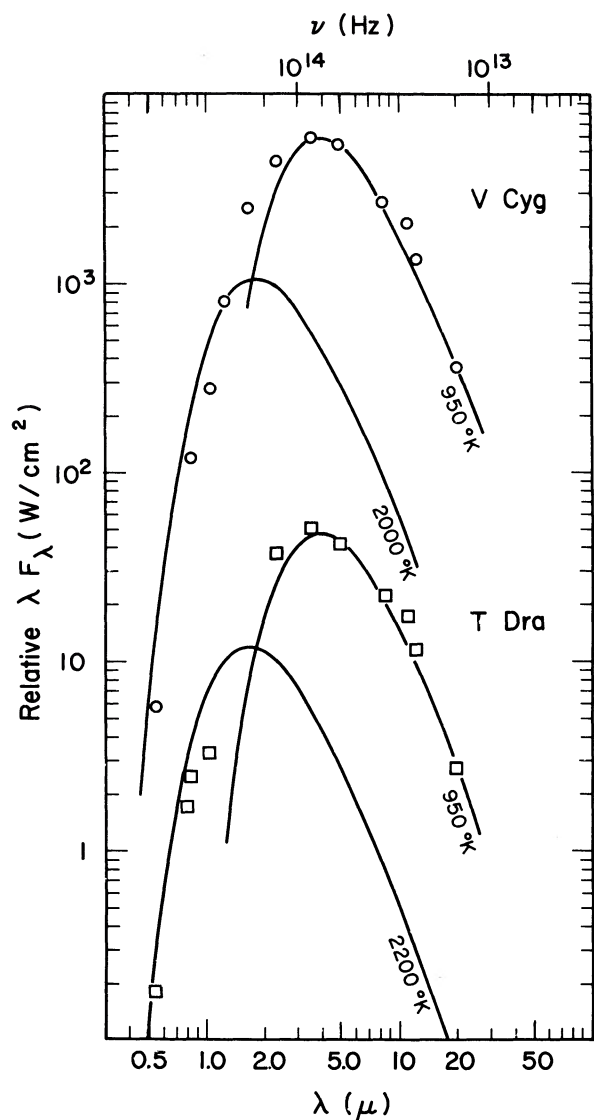


FIG. 13.—Energy distribution of the carbon stars T Dra and V Cyg. The 2.3–12.5  $\mu$  data are from the present work. The other data have been adapted (with respect to visual phase) from the following sources: 20  $\mu$ : Morrison and Simon (1973). 1.25  $\mu$  and 1.65  $\mu$ : Frogel and Hyland (1972). 1.04  $\mu$ : Baumert (1972). 0.84  $\mu$ : Neugebauer and Leighton (1969). V: Mayall (1973).

of carbon stars is characterized by a smooth continuum with a possible downturn for  $\lambda < 8 \mu$  and a superposed emission feature in the range  $\sim 10$ –12.5  $\mu$ . The energy distribution of the semiregular variables indicates that the continuum is due primarily to stellar radiation, but for the Mira variables and V Hya the entire continuum at wavelengths beyond 8  $\mu$  probably represents excess over the star's radiation. This point will be discussed later. As an example of the observed energy distribution, a spectrum of the total flux from V Cyg is plotted in figure 12. For V Cyg the

observed spectrum is almost entirely excess over the stellar continuum (fig. 13). In order to compare the spectral distribution of the additional feature observed over the 10–12.5  $\mu$  wavelength range in various carbon stars a blackbody has been fitted to the observed continuum and subtracted. The result of this procedure for V Cyg, T Dra, R Lep, V Hya, UU Aur, and IRC+10216 is shown in fig. 12. In addition, to improve the statistical significance, the excess spectra for V Cyg, T Dra, R Lep, and V Hya have been normalized and averaged together. The error bars represent the statistical errors obtained. The shape of the distribution is quite different from the silicate distribution typical of M stars, and it has been suggested that this feature be identified with silicon carbide grains (Treffers and Cohen 1974; Gilra 1972*a, b*).

The photometric energy distribution of the carbon Mira variables V Cyg and T Dra are shown in figure 13. It is not possible to fit a single-temperature blackbody spectrum to these stars in any reasonable way, although this can be done in the case of most other stars. It seems appropriate in the context of the present discussion of excess radiation from grains to point out the possibility that most of the radiation at wavelengths longer than 2  $\mu$  from V Cyg and T Dra is due to a circumstellar shell at an apparent temperature of approximately 900° K. The grains might have significant emissivity at all wavelengths such as would be expected from "blackbody" grains, in contrast to those particles having large emissivity over only a narrow range of wavelengths such as silicate grains. If this hypothesis were correct, the excess radiation indicated by the silicon carbide feature in the 8–14  $\mu$  spectral region would represent a small fraction of the total excess radiation from circumstellar grains for these stars. Frogel and Hyland (1972) have shown that the 2.3- $\mu$  absorption of CO is weaker in carbon Mira stars than in non-Mira variables. This was interpreted as a filling in of CO bands by circumstellar emission of grains in support of the above interpretation. In contrast, the energy distribution of the semiregular variables UU Aur, Y Tau, and Y CVn indicates little if any excess "blackbody" continuum, yet the silicon carbide feature is quite distinct. The ratio silicon carbide/blackbody excess appears to be greatly variable among carbon stars.

In summary, the characteristic silicate excess emission appears in the energy distribution of many M and S stars. Some of these spectra are not identical with that of the material in the Orion Trapezium region. The effects of mixtures of grains of different types of silicates, optical depth, particle size, and possible differences in the stellar continuum must be investigated further. Whenever a large excess is observed—e.g.,  $\mu$  Cep, R Cas, R W Cyg—the excess is observed to be quite similar to the Trapezium. The excess radiation from the carbon stars originates in grains that produce an underlying continuum showing little variation of emissivity with wavelength such as graphite along with a characteristic excess between 10 and 12.5  $\mu$  attributable to silicon carbide.

## VI. CONCLUSIONS

As a result of the study of the variability of cool stars at infrared wavelengths, the following conclusions are drawn:

1. There is no evidence that the changes in intrinsic polarization of starlight can be attributed to a significant change in the total amount of circumstellar dust. Infrared emission is interpreted in terms of the large-scale emission of grains around the star—perhaps condensing and being blown out through the gas by radiation pressure as discussed by Gilman (1972). The changes in intrinsic polarization should be interpreted in terms of scattering and absorption by much more localized and transient regions of gas and dust.

2. There is some evidence, from the dependence of the observed  $[11\ \mu] - [8.4\ \mu]$  color with phase compared with that expected due to a constant amount of dust heated by a variable stellar luminosity and temperature, that perhaps on average there is more circumstellar dust at minimum phase than at maximum phase. This evidence is indirect in that no  $[11\ \mu] - [8.4\ \mu]$  color change has been observed whereas a decrease in this color is expected at minimum phase due to a decrease in the stellar luminosity and temperature.

3. There is no evidence for changes with time of circumstellar dust surrounding carbon stars.

The data that have been obtained on the spectral

energy distribution of excess radiation from stars indicate that:

1) The characteristic "silicate" type emission profile similar to that observed from the Orion Trapezium region is found in many M and S stars. Some variations in detailed shape are found. Effects of optical depth and grain temperature do not sufficiently explain these variations. Large grain size can apparently effectively influence the shape of the observed spectrum. This matter will be investigated further.

2) The excess emission from carbon stars can probably be attributed to radiation characteristic of the emissivity with wavelength of silicate carbide grains superposed on a blackbody continuum. The amount of blackbody excess is much stronger from carbon Mira variables than from semiregular variables.

3) No spectra have been observed in this investigation that would require interpretation in terms of grains of exceedingly different chemical composition than those discussed—blackbody grains, silicate grains, and silicon carbide grains.

The authors wish to acknowledge discussions and assistance by K. M. Merrill and unpublished polarization data contributed by H. M. Dyck, S. J. Shawl, and K. Serkowski. This work has been supported by the National Aeronautics and Space Administration and the National Science Foundation.

## REFERENCES

- Baumert, J. H. 1972, Ph.D. thesis, Ohio State University.  
 Campbell, L. 1955, *Studies of Long Period Variables* (Cambridge, Mass.: AAVSO).  
 Dombrovskii, V. A. 1970, *Astrofizika*, **6**, 207.  
 Dyck, H. M. 1968, *A.J.*, **73**, 688.  
 Dyck, H. M., Forrest, W. J., Gillett, F. C., Stein, W. A., Gehrz, R. D., Woolf, N. J., and Shawl, S. J. 1971, *Ap. J.*, **165**, 57.  
 Dyck, H. M., and Sanford, M. T. 1971, *A.J.*, **76**, 43.  
 Dyck, H. M., and Shawl, S. J. 1972, unpublished observations.  
 Frogel, J. A. 1971, Ph.D. thesis, California Institute of Technology.  
 Frogel, J. A., and Hyland, A. R. 1972, *Mém. Soc. Roy. Sci. Liège*, Ser. 3, p. 111.  
 Gammon, R. H., Gaustad, J. E., and Treffers, R. R. 1972, *Ap. J.*, **175**, 687.  
 Gillett, F. C., and Forrest, W. J. 1973, *Ap. J.*, **179**, 483.  
 Gillett, F. C., Low, F. J., and Stein, W. A. 1968, *Ap. J.*, **154**, 677.  
 Gillett, F. C., Merrill, K. M., and Stein, W. A. 1971, *Ap. J.*, **164**, 83.  
 Gilman, R. C. 1972, *Ap. J.*, **178**, 423.  
 Gilra, D. P. 1972a, *The Scientific Results from the Orbiting Astronomical Observatory*, NASA SP-310, p. 295.  
 ———. 1972b, *Interstellar Dust and Related Topics*, IAU Symposium No. 52, ed. J. M. Greenberg and H. C. van de Hulst, to be published.  
 Hackwell, J. A. 1971, Ph.D. thesis, London University College.  
 ———. 1972, *Astr. and Ap.*, **21**, 239.  
 Kruszewski, A., Gehrels, T., and Serkowski, K. 1968, *A.J.*, **73**, 677.  
 Kukarkin, B. V., Kholopov, P. N., Efremov, Yu. N., Kukarkina, N. P., Kurochkin, N. E., Medvedeva, G. I., Perova, N. B., Fedorovich, V. P., and Frolov, M. S. 1969, *General Catalog of Variable Stars* (Moscow: Academy of Sciences of USSR).  
 Mayall, M. W. 1973, AAVSO Observations, private communication.  
 Morrison, David, and Simon, Theodore. 1973, *Ap. J.*, **186**, 193.  
 Neugebauer, G., and Leighton, R. B. 1969, *Two Micron Sky Survey* (Washington: NASA).  
 Ney, E. P., Strecker, D. W., and Gehrz, R. D. 1973, *Ap. J.*, **180**, 809.  
 Serkowski, K. 1966, *Ap. J.*, **144**, 857.  
 ———. 1971a, *Contr. Kitt Peak Obs.*, No. 554, p. 107.  
 ———. 1971b, *Veröff. Remeis Sternw. Bamberg*, **9**, 11.  
 ———. 1974, unpublished observations.  
 Shawl, S. J. 1971, *Bull. AAS*, **3**, 442.  
 ———. 1972, Ph.D. thesis, University of Texas.  
 Spinrad, H., and Newburn, R. L. 1965, *Ap. J.*, **141**, 965.  
 Stein, W. A., and Gillett, F. C. 1969, *Ap. J. (Letters)*, **155**, L197.  
 Strecker, D. W. 1973, Ph.D. thesis, University of Minnesota.  
 Treffers, R., and Cohen, M. 1974, *Ap. J.*, in press.  
 Vardanian, R. A. 1969, *Non-Periodic Phenomena in Variable Stars*, ed. L. Detre (Budapest: Academic Press), p. 339.  
 Woolf, N. J., and Ney, E. P. 1969, *Ap. J. (Letters)*, **155**, L181.  
 Woolf, N. J., Schwarzschild, M., and Rose, W. K. 1964, *Ap. J.*, **140**, 833.  
 Zappala, R. R. 1967, *Ap. J. (Letters)*, **148**, L81.

W. J. FORREST: Department of Physics, University of California, San Diego, P.O. Box 109, La Jolla, CA 92037

F. C. GILLETT: Kitt Peak National Observatory, P.O. Box 26732, Tucson, AZ 85726

W. A. STEIN: Department of Physics, University of California, San Diego, P.O. Box 109, La Jolla, CA 92037; and School of Physics and Astronomy, University of Minnesota, Minneapolis, MN 55455